The Behavior of Radiogenic Particles at Solidification Fronts

Francisco J. Arias[a,b], Geoffrey T. Parks[b*]
[a] *Department of Fluid Mechanics, University of Catalonia, ESEIAAT C/ Colom 11, 08222 Barcelona, Spain and*
[b] *Department of Engineering, University of Cambridge, Trumpington Street, Cambridge CB2 1PZ, United Kingdom*
(Dated: November 21, 2016)

The thermal behavior of insoluble radiogenic particles at the solid-liquid interface of an advancing solidification front and its significance with regard to environmental impact are discussed. It is shown that, unlike classical particles, where the most probable behavior is engulfing by the solidification front, radiogenic particles are more likely to be rejected by the solidification front. Utilizing a simplified physical model, an adaptation of classical theoretical models is performed, where it is shown that, unlike classical particles, for radiogenic particles the mechanism is thermally driven. An analytical expression for the critical velocity of the solidification front for engulfing/rejection to occur is derived. The study could be potentially important to several fields, e.g. in engineering applications where technological processes for the physical removal of radionuclide particles dispersed throughout another substance by inducing solidification could be envisaged, in planetary science where the occurrence of radiogenic concentration could result in the possibility of the eruption of primordial comet/planetoides. Finally, for specific cases, particle ejection may result in an increase of concentration as the front moves which can translates in the formation of radiative hallos or hot spots.

Keywords. *Radiogenic particles, solidification, planetary science*

I. INTRODUCTION

To date the study of particle behavior at solidification fronts has been of practical importance in several different areas of science, for example: biological, soil, food and metallurgy. Unfortunately, despite the abundant available literature, see for example (Li et al., 2010), there are no studies about the behavior of radiogenic particles. Such particles act as heat sources, and thus the topic requires theoretical development.

In this paper, a theoretical model for the behavior of particles at freezing fronts, but adapted to account for the heat source from radiogenic particles, is assessed. The theoretical model, although a simplified one, allows us to gain a first insight into the impact of the perturbed temperature profile surrounding radiogenic particles on the critical velocity which determines the likelihood of their being either engulfed or ejected by the solidification front. This should not be misconstrued as an attempt to produce a definitive mechanistic model of the behavior of such particles at solidification fronts, here only thermal effects are considered. Nonetheless, we feel that it is appropriate to start to air the topic in view of unavailable theory as far as the authors know, and then to encourage a thorough research of the subject.

*Corresponding author: Tel.: +93 73 98 666; Electronic address: frarias@mf.upc.edu

II. THEORETICAL BACKGROUND

The behavior of particles at solidification fronts has been extensively researched over several decades, and multiple aspects analyzed: see (Lipp et al., 1992; Coupard et al., 1996; Rempel and Worster, 1999; Garvin and Udaykumar, 2004; Garvin et al., 2007; Agaliotis et al., 2012; Kintea et al., 2016), just to name a few. A comprehensive review can be found in (Li et al., 2010). In this paper, by radiogenic particles we understand entities having diameters around 0.1 to 10 micrometers. Such particles in rivers or lakes with typical fluid velocities less than centimeter per second, feature very low Stokes numbers $\mathbf{Stk} \ll 1$ and then they follow fluid streamlines closely (perfect advection), i.e., will not settle due to gravity. These radionuclides particles are known to occur in the environment by mechanical disruption, pulverization and dispersion of the original bulk of radioactive material; condensed aggregates formed upon condensation of volatile radionuclides; discrete radioactive particles or clusters formed within the fuel during normal operations, IAEA, 2011
. To introduce the theory of the behavior of particles at solidification fronts, Fig. 1 shows a schematic representation of the two possibilities that can occur, depending on the velocity of solidification of the solidification front (Li et al., 2010). Referring to this figure, it can be seen that the behavior is not trivial. When the solidification front approaches a particle, the particle can be rejected or engulfed by the front. The behavior will depend on the velocity of the solidification front V. If the solidification front moves with a velocity lower than a certain

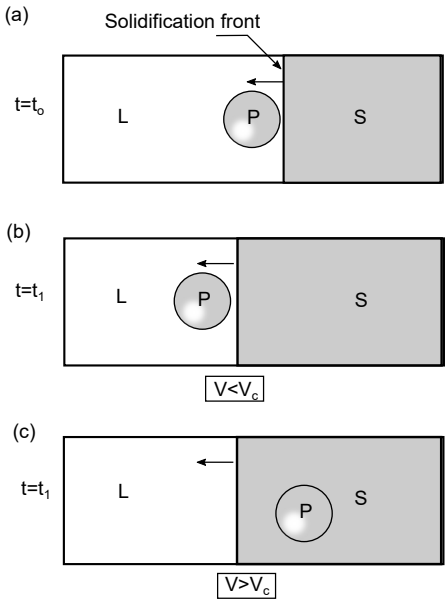

FIG. 1: Schematics of the behavior of a particle at a solidification front moving from right to left [courtesy of (Li et al., 2010)].

velocity called the critical velocity V_c, the particle will be rejected or pushed ahead of the front. However, if the solidification front moves with a velocity greater than V_c, the particle will be engulfed.

The critical velocity at which continuous rejection of particles occurs is given by (Li et al., 2010):

$$V_c = \frac{A_h(1-\nu)}{36\pi\mu R l_o} \tag{1}$$

where A_h is the Hamaker coefficient, ν is the ratio of the particle radius to the radius of curvature of the concave solid-liquid interface, μ is the liquid viscosity, R is the radius of the particle, and l_o is the minimum separation distance between the particle and the solid. The minimum separation distance for small particles is given by:

$$l_o = 1.3\left[\frac{A_h R}{12\pi\gamma}\right]^{\frac{1}{3}} \tag{2}$$

where γ is the interface surface tension. Therefore, Eq. (1) may be rewritten as:

$$V_c = 0.049\left[\frac{\gamma A_h^2}{\pi^2 R^4}\right]^{\frac{1}{3}}\frac{(1-\nu)}{\mu} \tag{3}$$

If the solidification front is perfectly flat, $1-\nu \simeq 1$ and Eq. (3) simplifies to:

$$V_c = 0.049\left[\frac{\gamma A_h^2}{\pi^2 R^4}\right]^{\frac{1}{3}}\frac{1}{\mu} \tag{4}$$

However, it was found that the relative interface concavity is dependent upon the relative values of the thermal conductivities of the particle and the matrix material (Chernov et al., 1976), and the drag on a particle being pushed by a solidification front and its dependence on thermal conductivities was studied by (Garvin and Udaykumar, 2004). It was found that the concavity term is related to thermal conductivities by:

$$1-\nu = \frac{\kappa_p}{\kappa_l} \tag{5}$$

where κ_p and κ_l are the thermal conductivities of the particle and the liquid, respectively. Thus, inserting Eq. (5) into Eq. (3) one obtains:

$$V_c = 0.049\left[\frac{\gamma A_h^2}{\pi^2 R^4}\right]^{\frac{1}{3}}\frac{1}{\mu}\frac{\kappa_p}{\kappa_l} \tag{6}$$

As is readily apparent, the effect of the relative thermal conductivities could be very important in the rejection/engulfing process in increasing or decreasing the critical velocity for rejection by an order of magnitude. For example, the value of $\kappa_{\text{ceramic}}/\kappa_{\text{water}}$ is around 10 (e.g. $\kappa_{\text{C}}/\kappa_{\text{water}} = 10.2$ or $\kappa_{\text{TiO}_2}/\kappa_{\text{water}} = 12.3$), while the ratio is around 1 for systems like mica/water (e.g. $\kappa_{\text{mica}}/\kappa_{\text{water}} = 0.92$ or $\kappa_{\text{glass}}/\kappa_{\text{water}} = 1.25$) (Agaliotis et al., 2012)

The solid-liquid interface temperature is given by:

$$T_i = T_m - \left(\frac{\lambda}{d}\right)^3 T_m \tag{7}$$

and defining the difference of temperature between the front and the particle as $\Delta T_c = Tm - Ti$

$$\Delta T_c = \left(\frac{\lambda}{d}\right)^3 T_m \tag{8}$$

where T_m is the temperature at the solidification front, d is the thickness of the liquid film interface, and λ is a length scale proportional to the interaction strength (Rempel and Worster, 1999).

III. THE RADIOGENIC EFFECT

The preceding theory, however, ignores heat sources, and the particle and the surrounding liquid are taken to be at the same temperature. For radiogenic particles, this assumption is no longer appropriate. The heat released in the decay of the radiogenic particle distorts the temperature profile of the local liquid and thus will affect the critical velocity, as we will immediately see below.

First and foremost, the most important direct effect of the particle heat source on the calculated critical velocity is on the solid-liquid interface concavity $1-\nu$.

As can be envisaged by looking at Fig. 2, it is expected that the solid-liquid interface will become less concave (i.e. $[1-\nu] \rightarrow 1)]$) as the temperature of the particle increases, and, then according to the accepted theory, this will result in a higher critical velocity. Therefore,

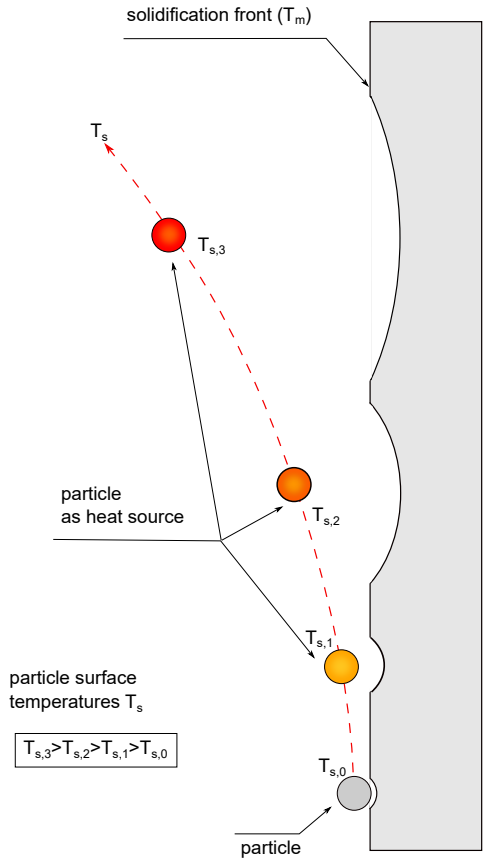

FIG. 2: The effect of the surface temperature of the particle on the solid-interface concavity.

the assumption of a flat solidification front, as depicted in Fig. 1, is also untenable, as the temperature profile is now locally distorting the shape of the solidification front.

The modified situation when considering a radiogenic particle as a heat source is now as given in Fig. 3.

Referring to Fig. 3, the curvature of the solidification front is disturbed by the heat from the radiogenic particle, and its profile is defined by the temperature difference between the surface of the radiogenic particle, let us denote this T_s, and the temperature at the solidification front T_m.

For the sake of simplicity, let us consider a spherical particle. Assume a heat flux q_p at the particle surface, i.e. at $r = R$, (a Neumann boundary condition), while the specified temperature at the solidification front is T_m when $r = R_m$ (a Dirichlet boundary condition). With these boundary conditions, solving the heat conduction equation in spherical coordinates with azimuthal and poloidal symmetry for the steady-state case, one obtains the following expression for T_s, the temperature at

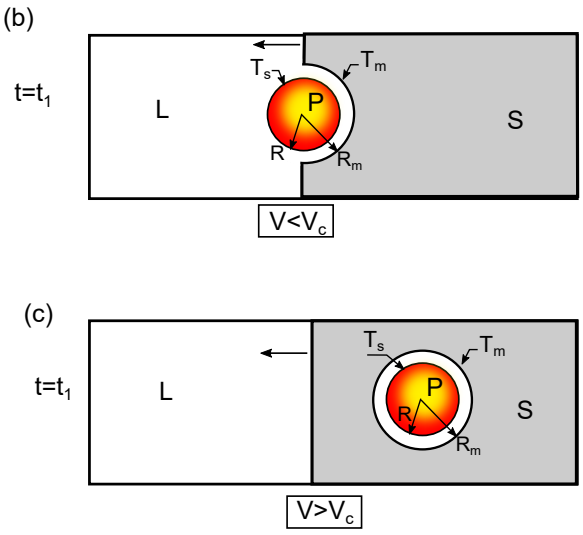

FIG. 3: Schematics of the behavior of a radiogenic particle at a solidification front moving from right to left.

the surface of the particle:

$$T_s = \frac{q_p R^2}{\kappa_l}\left(\frac{1}{R} - \frac{1}{R_m}\right) + T_m \tag{9}$$

The rate of heat production per unit volume, Q_p, in a radiogenic particle, for the simple case of a single radioactive component decaying to a stable daughter product, is given by:

$$Q_p = B_p \rho_p e_d \tag{10}$$

where B_p is the specific activity of particle (Bq/kg), ρ_p its density and e_d the decay energy. Using the fact that in steady state:

$$\frac{4}{3}\pi R^3 Q_p = 4\pi R^2 q_p \tag{11}$$

Using Eqs. (10) and (11), Eq. (9) can be rearranged to give:

$$\frac{1}{3} R^3 B_p \rho_p e_d = \kappa_l \Delta T \cdot \left[\frac{R}{1 - \frac{R}{R_m}}\right] \tag{12}$$

where $\Delta T = T_s - T_m$ is the temperature difference between the particle surface at $r = R$ and the solidification front at $r = R_m$. Thus, the parameter $1 - \nu = 1 - \frac{R}{R_m}$ is, for this case, thermally controlled, and is given by:

$$1 - \nu = \frac{3\kappa_l \Delta T}{R^2 B_p \rho_p e_d} \tag{13}$$

Substituting in Eq. (3), the expression for the critical velocity is then:

$$V_c^t = 0.049 \left[\frac{\gamma A_h^2}{\pi^2 R^4}\right]^{\frac{1}{3}} \frac{1}{\mu} \frac{3\kappa_l \Delta T}{R^2 B_p \rho_p e_d} \tag{14}$$

where the superscript t indicates that the process is thermally controlled to differentiate it from the classical critical velocity without heat source expression in Eq. (6). Dividing Eq. (14) by Eq. (6) one obtains:

$$\frac{V_c^t}{V_c} = 3\frac{\kappa_l^2}{\kappa_p}\frac{\Delta T}{R^2 B_p \rho_p e_d} \tag{15}$$

The thermal conductivities of the particle as well as the liquid can be assumed as constant. The only parameters which are unknown are the heat source and the ΔT. However they could be connected by considering a simple balance of energy. In fact, the surface heat flux of the particle is given by (Turcotte and Schubert, 2014):

$$q_p = \frac{1}{3} R B_p \rho_p e_d \tag{16}$$

The above equation is easily derived by combining Eqs. (10) and (11).

On the other hand the surface heat flux is given by

$$q_p = h_l \Delta T \tag{17}$$

where h_l is the heat transfer coefficient of liquid. Combining Eq.(17) with Eq.(16) one obtains

$$\frac{1}{h_l} = \frac{3\Delta T}{R B_p \rho_p e_d} \tag{18}$$

and inserting Eq.(18) into Eq.(15) yields

$$\frac{V_c^t}{V_c} = \frac{\kappa_l^2}{\kappa_p}\frac{1}{R h_l} \tag{19}$$

thee heat transfer coefficient for a specific system could be evaluated with its specific Reynolds numbers **Re** as $h_l \simeq aRe^n$ where $\mathbf{Re} = \frac{UL}{\nu_l}$ where U, L and ν_l are the velocity, length scale and kinematic viscosity of the liquid., respectively. For most cases, $a \sim 0.023$ and $n \sim 0.8$, being identically equal for the Dittus-Boelter correlation. In application to ice cover lakes, we have, (Matti, 2015): $U \sim 10^{-3}$m/s, the kinematic viscosity of water $\nu_l \approx 1.8 \times 10^{-6}$m^2/s and $L \sim 1 - 10$m resulting in a Reynolds number on $\mathbf{Re} \sim 5500$ and a heat transfer coefficient $\sim$22 W/(m^{2}K). Therefore, with the size of particles we are dealing ($\sim$ a few micrometers), the radiogenic particle is more prone to be rejected rather than engulfed by the front of solidification. It should be noted the strong dependence with the radius of particle. Even accepting that the discussed result is based in entirely thermal considerations and other possible effects, as ionization, electrostatic charges, etc., are not being considered, nevertheless the model provide an adequate physical picture of the behavior should be observed if only thermal effect were present, so if such effect is not observed in a particular experiment, this actually could betray the presence of other forces to be considered.

Finally, it is important to stress, that Eq.(19) is under the assumption that the difference of temperature ΔT is not identically zero and in fact is higher than the difference of temperature given by the classical model without heat sources Eq.(7). So, we can get an idea on the thermal strength by comparing both temperatures as follows:

First, the specific activity may be expressed as function of the half-life and molar mass of the radioisotope as

$$B_p = \frac{N_A}{\bar{M}}\frac{\ln 2}{t_{1/2}} \tag{20}$$

where N_A is the Avogadro number, $\bar{M}$ is the molar mass, and $t_{1/2}$ the half-life. From Eq.(18) we have

$$\Delta T = \frac{\ln 2 N_A \rho_p e_d}{3\bar{M} h_l}\frac{R}{t_{1/2}} \tag{21}$$

The difference in temperature without heat sources (classical particles) is given by Eq.(7). The interaction strength length λ is generally much greater than the molecular diameter of water. Under typical conditions $\lambda \approx 10^{-4}\mu$m, and $l \approx 10^{-2}\mu$m (Rempel and Worster, 1999), and taking $T_m \approx 300$ K, we obtain a $\Delta T_c \approx 10^-4$ K. We may define a thermal strength factor Γ as the ratio between the difference of temperature given by Eq.(21) and Eq.(8) as

$$\Gamma = \frac{\Delta T}{\Delta T_c} \tag{22}$$

which provide us an idea of when the heat from the radiogenic particle begin to be important.

Although the ΔT given by Eq.(21) must be evaluated for the specific radioisotope, however, the most significant effect is on the half-life $t_{1/2}$. In fact, densities could vary as much as a factor 3 the energy of decay is the order of 1 MeV to 5 MeV, and the molar mass also a factor 10 or so. For the sake of illustration, we take some average values of several parameters of the radiogenic particle assuming: $\rho_p \sim 4000$kg/m^3; $e_d \sim 2.5$ MeV; $\bar{M} \sim 200$gr/mol, and $\sim$22 W/(m^{2}K). The resulting curve for the parameter Γ, taking a radius of the particle around 5μm, is shown in Fig. 4. It is easy to see, that for particles with $t_{1/2} < 10^4$ years, the heat form the radiogenic source begin to be important.

A. Electrostatically charged particles and ions

It is important to highlight that in the preceding study only the thermal impact of general radiogenic particles has been considered, and they were assumed to be neutral particles (i.e. to have no net electrical charge). However,

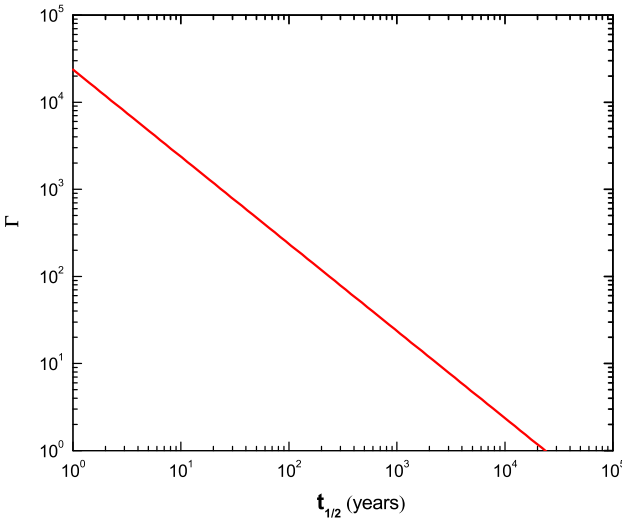

FIG. 4: Γ as function of half-life $t_{1/2}$ for the generic parameters assumed.

it should be noted that radiogenic particles could be either electrostatically charged (mostly positively charged) or could cause the formation of ions.

In the former case, electrostatic forces induced between the surface particle and the solidification front can be stronger than adhesive dipolar forces, and then whether the particle is rejected or engulfed will depend on whether the induced electrostatic field between the particle and the solidification front surface is repulsive or attractive.

In the latter case, i.e. if the radiogenic particle ionizes its neighborhood, according to classical theory on the effect of ions on the solidification process, a local freezing point depression, in which ions decrease the freezing point of the liquid, could be expected, and then the solid-liquid interface becomes less concave, resulting in a higher critical velocity.

Additional R&D is required in order to assess the behavior of solidification fronts affected by self-induced electrostatic fields and/or local ionization of the film between particle and solidification front.

IV. SUMMARY OF RESULTS AND CONCLUSIONS

The theory of the behavior of particles at solidification fronts has been revised to account for radioactive particles as heat sources. Some interesting questions are raised by this study:

(a) The motion of radiogenic particles at solidification fronts is a thermally controlled process, where the most probable outcome seems to be the rejection of radiogenic particles.

(b) As a result of the rejection of radiogenic particles, there will be an accumulation of radiogenic material at the solidification front.

(c) An analytical expression, Eq. (15), is derived for the critical velocity of engulfing, where the classical expression is modified by the thermal perturbation of the radiogenic particle, which distorts the shape of the solidification front as well as the distance between particle and front.

NOMENCLATURE

A_h = Hamaker coefficient
B_p = specific activity of radiogenic particle (Bq/kg)
c = concentration of radionuclide
d = thickness of the liquid film interface
h_l = heat transfer coefficient of liquid
h_o = energy production rate per unit volume due to radiogenic particles
l_o = minimum separation distance between particle and solidification front
q_p = heat flux at the particle surface
Q_p = particle heat generation rate
r = transverse distance from the solidification front
R = radius of the radiogenic particle
R_m = distance of the solidification front from the center of the radiogenic particle
Re = Reynolds number
$t_{1/2}$ = half-life of radiogenic particle
v_p = velocity of solidification
V_c = critical velocity for engulfing
Stk = Stokes number
t = time
T = temperature
T_m = solidification front temperature
T_o = environmental temperature
T_s = temperature of particle surface
ΔT = temperature difference between solidification front and particle

Greek symbols

ϵ_d = energy released per disintegration (MeV)
γ = surface tension
Γ = thermal strength factor
ρ_p = density of particle
μ = dynamic viscosity of the liquid
η = radionuclide mineral fraction
κ_l = thermal conductivity of liquid
κ_p = thermal conductivity of particle
λ = length scale
λ = decay constant
μ = dynamic viscosity of liquid
ν = ratio of particle radius to the radius of curvature of the concave solid-liquid interface

Subscripts

c = critical
l = liquid
p = particle

ACKNOWLEDGEMENTS

This research was supported by the Spanish Ministry of Economy and Competitiveness under fellowship grant Ramon y Cajal: RYC-2013-13459.

V. REFERENCES

Radioactive Particles In The Environment: Sources, Particle Characterization And Analytical Techniques. IAEA, Vienna, 2011 IAEA-TECDOC-1663

Agaliotis, E.M., Schvezov, C.E., Rosenberger, M.R., Ares, A.E., 2012. A numerical model study of the effect of interface shape on particle pushing. J. Cryst. Growth 354, 49–56

Ashley, S., 2001. Warp drive underwater. Sci. Am. 284, 70–79.

Chernov, A.A., Temkin, D.E., Melnikova, A M., 1976. Theory of the capture of solid inclusions during the growth of crystals from the melt. Sov. Phys. Crystallogr. 21, 369–374.

Coupard, D., Girot, F., Quenisset, J.M., 1996. Models describing the interaction of particles with a plane solid/liquid interface. J. Mater. Sci. 31, 5305–5308.

Garvin, J W., Udaykumar, H.S., 2004. Drag on a particle being pushed by a solidification front and its dependence on thermal conductivities. J. Cryst. Growth 267, 724–737.

Garvin, J.W., Yang, Y., Udaykumar, H.S. 2007. Multiscale modeling of particle–solidification front dynamics, Part I: Methodology. Int. J. Heat Mass Tran. 50, 2952–2968.

Kintea, D.M., Roisman, I.V., Tropea, C., 2016. Transport processes in a wet granular ice layer: Model for ice accretion and shedding. Int. J. Heat Mass Tran. 97, 461–472.

Li, D., Zuo, Y., Neumann, A.W., 2010. Behavior of particles at solidification fronts, in: Neumann, A.W., David, R., Zuo, Y. (Eds.), Applied Surface Thermodynamics, second ed. CRC Press, Boca Raton, pp. 633–697.

Lipp, G., Rödder, M., Körber, C., Rau, G., 1992. Preliminary investigations on the interaction of particles and icewater interfaces during bulk freezing. Cryo-Lett. 13, 229–238.

Rempel, A.W., Worster, M.G., 1999. The interaction between a particle and an advancing solidification front. J. Cryst. Growth 205, 427–440.

Turcotte, D.L., Schubert, G., 2014. Geodynamics. Third edition. Cambridge University Press, Cambridge, UK.

Matti Leppäranta Freezing of Lakes and the Evolution of their Ice Cover. Springer-Verlag Berlin Heidelberg. 2015